doi:10.1016/S0022-2836(02)00399-6 available online at http://www.idealibrary.com on IDEAL® J. Mol. Biol. (2002) 319, 1279–1290

JMB

Mutations that Reduce Aggregation of the Alzheimer's Aβ42 Peptide: an Unbiased Search for the Sequence Determinants of Aβ Amyloidogenesis

Christine Wurth, Nathalie K. Guimard and Michael H. Hecht*

Department of Chemistry
Princeton University
Princeton, NJ 08544, USA

The primary component of amyloid plaque in the brains of Alzheimer's patients is the 42 residue amyloid-β-peptide (Aβ42). Although the amino acid residue sequence of Aβ42 is known, the molecular determinants of Aβ amyloidogenesis have not been elucidated. To facilitate an unbiased search for the sequence determinants of Aβ aggregation, we developed a genetic screen that couples a readily observable phenotype in *E. coli* to the ability of a mutation in Aβ42 to reduce aggregation. The screen is based on our finding that fusions of the wild-type Aβ42 sequence to green fluorescent protein (GFP) form insoluble aggregates in which GFP is inactive. Cells expressing such fusions do not fluoresce. To isolate variants of Aβ42 with reduced tendencies to aggregate, we constructed and screened libraries of Aβ42–GFP fusions in which the sequence of Aβ42 was mutated randomly. Cells expressing GFP fusions to soluble (non-aggregating) variants of Aβ42 exhibit green fluorescence. Implementation of this screen enabled the isolation of 36 variants of Aβ42 with reduced tendencies to aggregate. The sequences of most of these variants are consistent with previous models implicating hydrophobic regions as determinants of Aβ42 aggregation. Some of the variants, however, contain amino acid substitutions not implicated in pre-existing models of Aβ amyloidogenesis.

Keywords: Alzheimer's disease; amyloid-β peptide variant; protein aggregation; amyloidogenesis; green fluorescent protein

*Corresponding author

Introduction

The deposition of insoluble protein fibrils is associated with a number of neurodegenerative diseases including Parkinson's disease, the prion-associated disorders (e.g. Creutzfeld–Jakob), and Alzheimer's disease.[1] In Alzheimer's disease, the primary component of these amyloid fibrils is the amyloid-β peptide (Aβ).[2,3] Aβ is generated *in vivo* by sequential proteolytic cleavage of the amyloid precursor protein (APP) by two proteolytic enzymes known as β and γ secretases. Because APP can be cleaved at several different sites, the ~4 kDa Aβ peptide is not a homogeneous product.[4] The most abundant forms found in amyloid plaque are a 40-mer and a 42-mer. These two forms, called Aβ40 and Aβ42, differ only by the latter containing the additional amino acid residues, Ile_{41} and Ala_{42}, at its C terminus. Although Aβ40 is produced in greater abundance, the slightly longer Aβ42 is more amyloidogenic and is the major component of neuritic plaques.[3,5]

Evidence that Aβ amyloidogenesis plays a causative role in the development of Alzheimer's disease is furnished by a variety of genetic, neuropathological and biochemical studies: All four of the genes that have been linked definitively to inherited forms of Alzheimer's disease increase the production and/or deposition of Aβ in the brain.[3,6] Moreover, recent studies have shown that drugs known to reduce the prevalence of Alzheimer's disease in epidemiological studies also reduce the levels of Aβ42 in cultured cells.[7] The correlation and co-localization of protein fibrils with tissue degeneration suggests that either the fibrils themselves, or precursors on the pathway

Abbreviations used: Aβ, amyloid-β peptide; APP, amyloid precursor protein; DMSO, dimethyl sulfoxide; GFP, green fluorescent protein; GM, green mutant; LB, Luria–Bertani medium; dNTP, deoxyribonucleoside triphosphate; PB, phosphate buffer; PBS, phosphate buffered saline; TFE, trifluoroethanol.

E-mail address of the corresponding author: hecht@princeton.edu

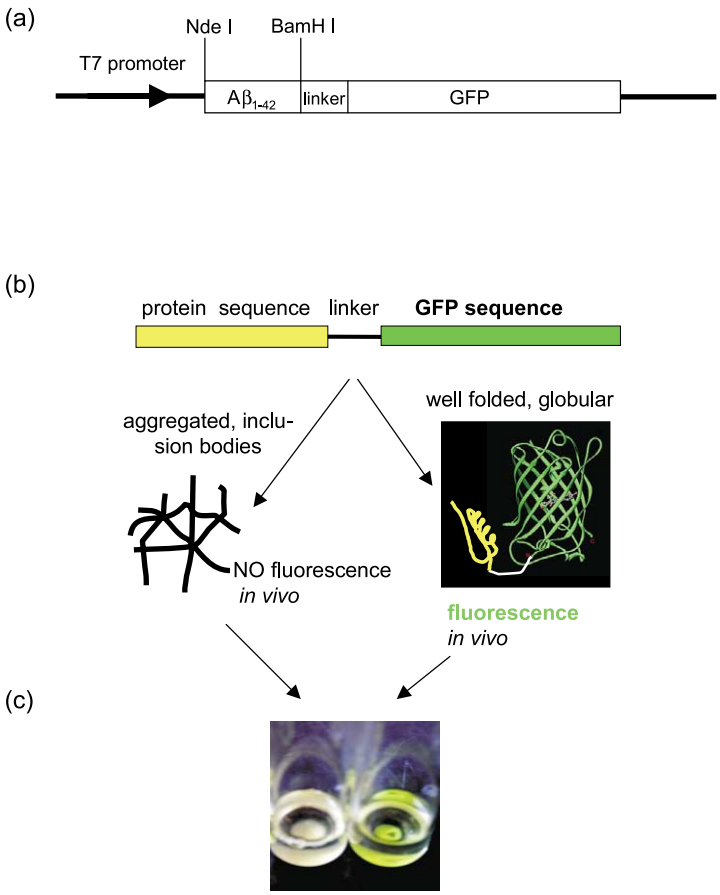

Figure 1. Screen for non-aggregating variants of Aβ42. (a) Gene encoding fusion proteins containing Aβ42 linked to green fluorescent protein (GFP). (b) Schematic depiction of the properties of Aβ–GFP fusion proteins. Wild-type Aβ42 forms insoluble amyloid (left) and prevents the GFP portion of the fusion protein from forming its native fluorescent structure. However, mutants in the Aβ42 sequence that prevent aggregation enable GFP to form its native green fluorescent structure (right). (Note: Structures of the Aβ variants are not known, and the yellow part of the ribbon diagram is merely a schematic cartoon.) (c) *E. coli* cells expressing GFP fusions to wild type (left) and mutant (right) forms of Aβ42. The wild-type Aβ42 causes the GFP fusion to form insoluble non-fluorescent aggregates. In contrast the mutant (GM6) diminishes aggregation and thereby enables the GFP reporter to form native green fluorescent protein.

towards fibrillogenesis play a critical role in the development of disease.[1,8–11] These and other studies led Koo *et al.*[1] to conclude "that inhibition of fibril formation could be a viable therapeutic strategy. Therefore, it is critical to develop an understanding of the process of fibril formation at a molecular level."

The initial purification of Aβ from amyloid deposits was reported in the mid 1980s[5,12,13] and the complete amino acid sequence has been known since 1987.[14] Nonetheless, it is not yet clear how this particular sequence drives Aβ to self-assemble into aggregated fibrillar structures. In more typical protein systems, the sequence determinants of protein structure and/or assembly are probed by two complementary approaches: structure determination and mutagenesis. Determination of a structure at atomic resolution enables one to observe directly how a particular amino acid sequence adopts a specific 3-dimensional structure. In the case of Aβ, however, high-resolution structural studies have been hampered by the fact that the physiologically relevant peptide Aβ42 aggregates in aqueous solution. Therefore, structural studies have focused either on Aβ solubilized in non-physiological solvents such as DMSO, TFE or SDS, or on fragments of Aβ that are less prone to aggregation.[15–20] The detailed structure of the fibrils themselves remains elusive, as the insoluble, non-crystalline fibrils are unsuitable for conventional methods for high-resolution structure determination (see Serpell[21] and Lynn & Meredith[22] for reviews).

Mutagenesis studies of Aβ also have been incomplete. Although a number of amino acid substitutions have been constructed and characterized in the Aβ42 peptide and/or in shorter fragments,[23–30] a large-scale screen for mutations that prevent amyloidogenesis has not been reported. The sequence substitutions studied in the past typically were designed to prove or disprove specific hypotheses about the roles of particular residues or regions of sequence. However, an unbiased screen for amino acid substitutions that prevent amyloidogenesis has not been possible hitherto because neither genetic selections *in vivo*, nor high-throughput screens *in vitro* have been available.

In the current study, we describe a model-independent strategy for isolating non-aggregating variants of Aβ42 from libraries of randomly generated mutants. The screen is based on our finding that N-terminal fusions of Aβ42 to green fluorescent protein (GFP) prevent proper folding of GFP in *E. coli*, and therefore do not fluoresce. The diminution of fluorescence in GFP fusions is known to correlate with the tendency of the N-terminal fusion partner to form insoluble aggregates.[31] To isolate sequence variants of Aβ42 with reduced tendencies to aggregate, we screened

libraries of Aβ42–GFP fusions in which the wild-type Aβ42 sequence had been replaced by randomly-generated mutants. Fusions with non-aggregating mutants of Aβ42 allow proper folding of the GFP reporter. Therefore, colonies expressing such mutants exhibit green fluorescence (Figure 1). Implementation of this screen facilitated isolation of a collection of 36 variants of Aβ42 that are more soluble and less prone to aggregate than the wild-type peptide.

Results

A screen for variants of Aβ42 with reduced amyloidogenicity

The development of a high throughput screen for non-amyloidogenic variants of Aβ42 requires that the solubility/aggregation behavior of Aβ be coupled to a readily observable property. Such coupling can be achieved by fusing the Aβ sequence to a reporter protein in such a way that correct folding (and hence function) of the reporter protein is blocked by Aβ aggregation, but enabled by mutations in Aβ that diminish aggregation.

Several methods have been described to link an easily monitored function in a reporter protein to the solubility/aggregation behavior of a fused protein or peptide.[31–33] The system described by Waldo *et al*.[31] uses GFP as the reporter. Formation of the GFP chromophore requires correct folding. Moreover, this process is slow (≥30 min), and fusion partners that aggregate into insoluble material interfere with the ability of GFP to achieve its native fluorescent structure.[31] In a systematic study using 20 different test proteins, Waldo *et al*. demonstrated that the fluorescence of *E. coli* cells expressing fusions to the N terminus of GFP correlated with the solubility of the test protein expressed alone (i.e. not fused to GFP).

We constructed a fusion protein in which GFP was linked to the C terminus of Aβ42. Synthetic oligonucleotides were used to construct a gene for wild-type Aβ42. This gene was then inserted in a vector provided by Geoffrey Waldo, upstream of the GFP sequence and under control of the T7 promotor. The Aβ42 sequence was separated from the GFP sequence by a 12 residue linker.[31] Pilot experiments demonstrated that *E. coli* cells express the wild-type Aβ42–GFP fusion at high levels; however, they do not fluoresce. Thus, the presence of the amyloidogenic Aβ42 sequence as an N-terminal fusion prevents GFP from forming its native fluorescent structure.

Mutagenesis of Aβ42

To facilitate an unbiased and model-independent assessment of which amino acid substitutions in Aβ42 prevent aggregation, we constructed libraries of mutants using random, rather than site-directed, mutagenesis. To circumvent the potential biases of any given method of mutagenesis, we used three different methods to construct three libraries of mutants: The first method, error prone PCR using *Taq* polymerase, produces random mutations, but is known to target AT base pairs more frequently than GC base pairs.[34] To circumvent potential biases associated with this method, we constructed a second library using the Mutazyme™ polymerase,[35] which is known to have the opposite target preference (it targets GC more frequently than AT). Finally, we constructed a third library of mutants that did not require incorporation of mismatched bases by an error-prone polymerase. This library was constructed by re-synthesizing the Aβ42 gene using 'doped' oligonucleotides in which each position was synthesized with 97% of the correct nucleotide and 1% of each of the other three nucleotides.

For all three libraries, mutagenesis was performed only on the DNA encoding Aβ42, not on the GFP fusion. Libraries of mutated Aβ42 sequences were cloned into the GFP fusion vector, and screened for green fluorescence.

Screening for Aβ variants

Aβ–GFP fusions constructed with mutated Aβ42 sequences were transformed into *E. coli* cells and plated. Colonies were then transferred to another plate to induce protein expression (see Materials and Methods). After three hours of induction, plates were visually scanned for green fluorescent colonies. The frequency of green colonies depended on the mutagenesis method, and ranged from ~1/100 (doped oligonucleotides) to ~1/5000 (Mutazyme). The intensity of the green color varied from mutant to mutant. Green colonies were picked and DNA was prepared for sequence analysis. The amino acid sequences of the Aβ42 variants that yielded green fusion proteins are shown in Figure 2 (green mutant, GM). *Taq* polymerase PCR produced GM1–20, Mutazyme™ PCR produced GM21–36, and the doped oligonucleotides produced GM43–79. Some of the variants contain single amino acid substitutions, while others contain multiple substitutions.

Fluorescence of Aβ–GFP fusions

The relative fluorescence intensities of *E. coli* cells expressing GFP fusions to the Aβ42 mutants are compared in Figure 3. Cells expressing the GFP fused to wild-type Aβ42 do not fluoresce. The dynamic range of fluorescence—comparing the most fluorescent mutant to wild-type Aβ42—is approximately 20-fold. The range among the mutants is ~fivefold (Figure 3).

Expression levels and solubility

We interpret the fluorescence of cells expressing mutant Aβ42 fused to GFP as indicating that these

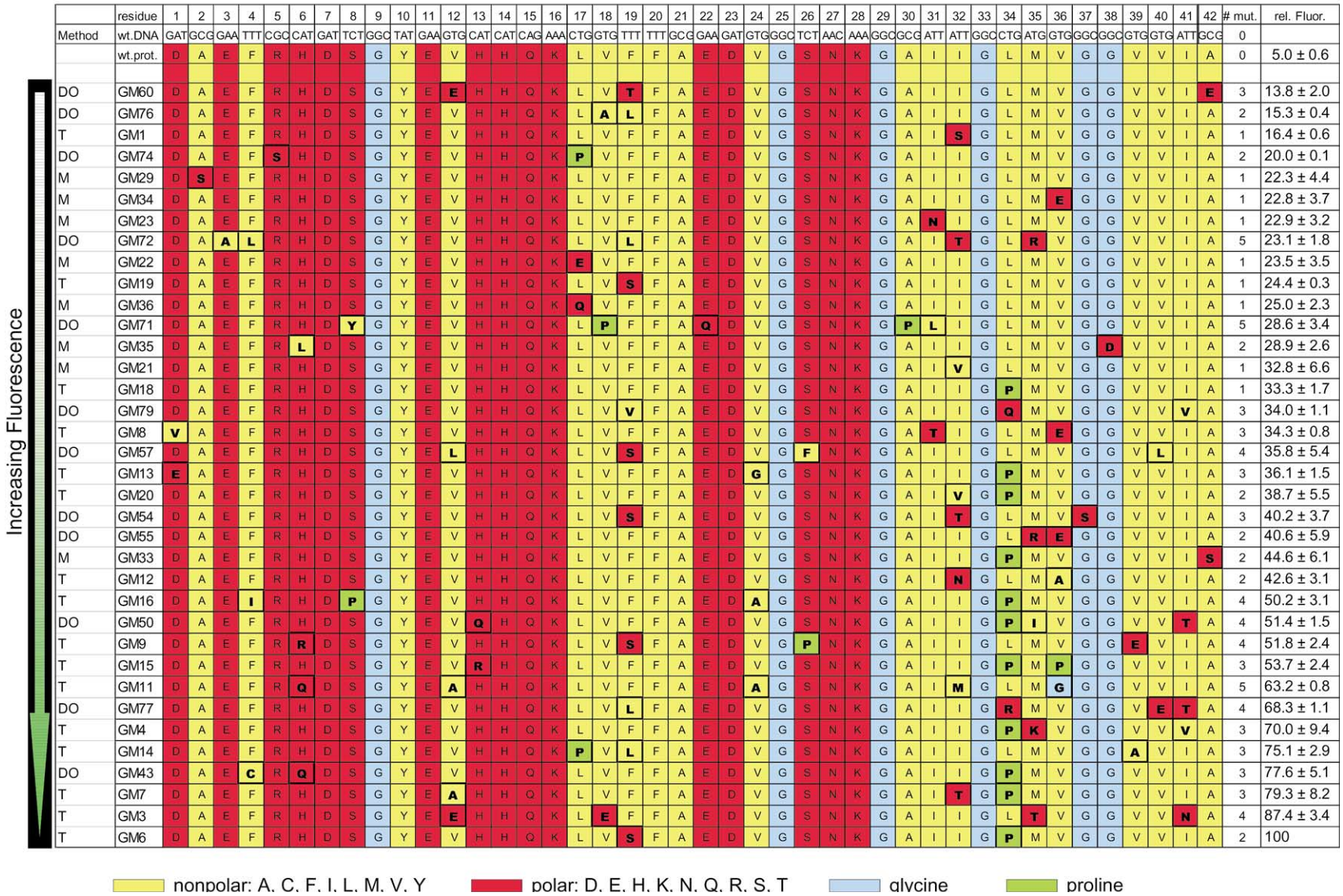

Figure 2. Sequences of variants of Aβ42 that reduce aggregation. The variants are ordered by increasing fluorescence intensity relative to GM6 (last column). Amino acid sequences are shown using the single letter code with nonpolar amino acid residues in yellow, polar amino acid residues in red, proline in green and glycine in blue. The mutagenesis methods by which the mutants were obtained are marked as "T" for *Taq* polymerase, "M" for Mutazyme polymerase and "DO" for doped oligonucleotides. The number of mutations per variant is listed at the right of each sequence.

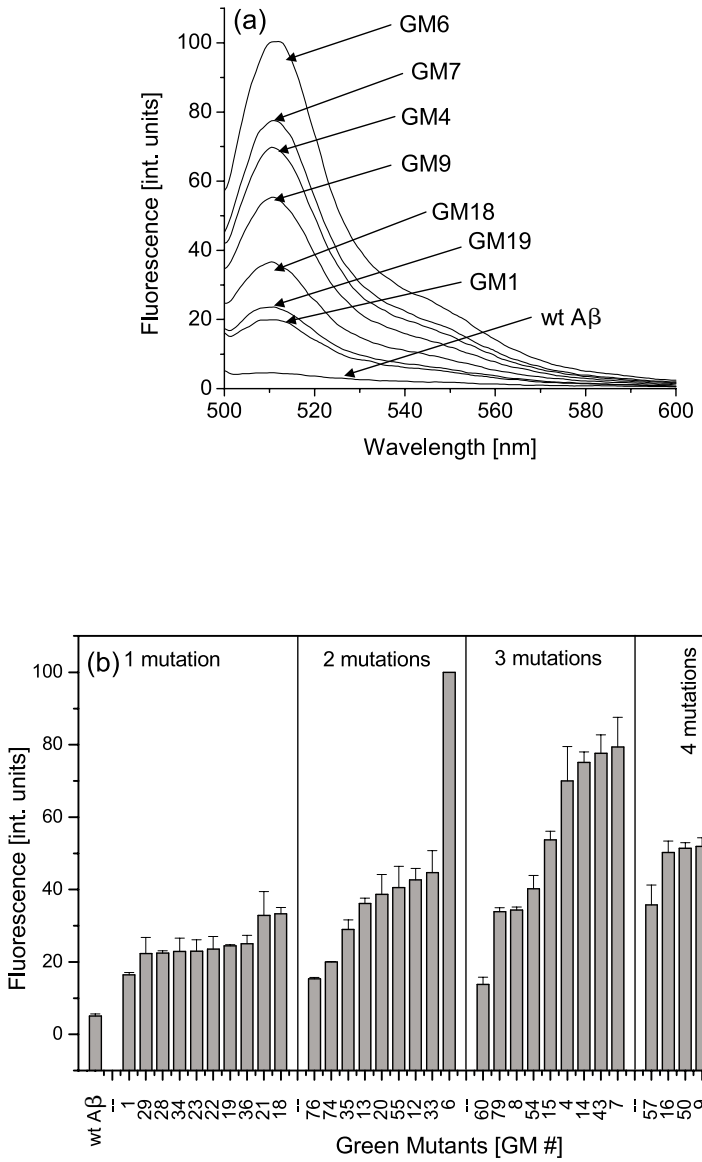

Figure 3. (a) Fluorescence spectra of *E. coli* cells expressing GFP fusions to wild type and mutant forms of Aβ42. Absolute fluorescence intensities at 510 nm ranged from 5.0 for wild-type Aβ42 to 97.9 for the mutant GM6. (b) Fluorescence data of *E. coli* expressing wild type and mutant forms of Aβ42 fused to GFP. The data are ordered by number of mutations and increasing fluorescence.

variants of Aβ have a diminished tendency to aggregate. Moreover, we infer that the amplitude of the observed fluorescence (Figure 3) indicates the degree of solubility conferred by the mutations. To justify this interpretation, it is imperative to show (i) that the wild type and mutant fusion proteins express at similar levels; and (ii) that the fluorescence of cells expressing these fusions correlates with the solubility of the Aβ42–GFP fusion proteins.

Expression levels of Aβ42–GFP fusions were monitored by SDS-PAGE of whole cells following induction of expression. As shown in Figure 4, all clones (wild type and mutants) express at comparable levels.

To assess whether the fluorescence of cells expressing the fusions indeed correlates with protein solubility, we separated the soluble and insoluble fractions of the *E. coli* cells, and assayed the amount of fusion protein in each fraction. As

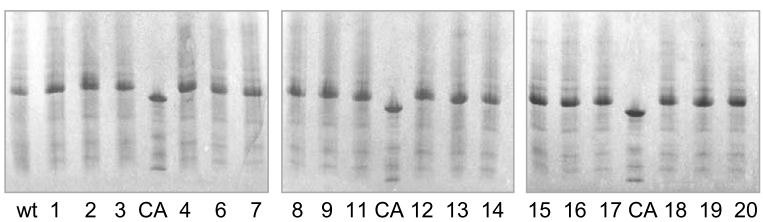

Figure 4. SDS-PAGE analysis of the expression levels of Aβ42 fusions to GFP shows that all mutants express the fusion proteins (M_r = 32 kDa) at similar levels; wt is wild-type Aβ42. The numbers 1–20 refer to mutants GM1–GM20 (sequences listed in Figure 2). Carbonic anhydrase (CA, M_r = 29 kDa) was used as a molecular mass marker.

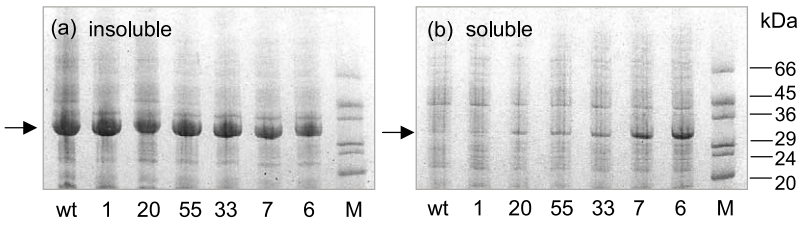

Figure 5. SDS-PAGE analysis of the solubility of wild type and mutant Aβ42 GFP fusions. (a) Insoluble fraction. (b) Soluble fraction. The wild-type Aβ42–GFP fusion occurs entirely in the insoluble fraction. Green fluorescent mutants partition into the soluble fraction. The greater the fluorescence signal (Figure 3) the more protein partitions into the soluble fraction. Arrows indicate the location of the Aβ42–GFP fusions at 32 kDa. M is a mixture of marker proteins (66, 45, 36, 29, 24 and 20 kDa).

shown in Figure 5, the fusion of GFP to wild-type Aβ42 occurs entirely into the insoluble fraction. In contrast, fusions to the Aβ42 mutants are seen in the soluble fraction. (For all samples, some material partitions into the insoluble fraction, as is frequently observed for recombinant proteins expressed at high levels in *E. coli*[36]) There is a good correlation between the amplitude of the fluorescence (Figure 3) and the amount of fusion protein in the soluble fraction (Figure 5). Thus the amplitude of the observed fluorescence (Figure 3) is a reasonable measure of the degree of solubility (or resistance to aggregation) conferred by the mutations.

An unbiased collection of Aβ42 variants

To assess whether our mutagenesis methods succeeded in producing an unbiased collection of mutations, we tabulated how often each type of DNA base change occurred in the collection. This tabulation is shown in Table 1 for each of the three libraries, and also for the collection as a whole. The overall collection—with mutants from all three libraries—contains mutations both at AT base pairs and at GC base pairs. Moreover, the collection contains an approximately equal number of transitions and transversions (59 *versus* 55). One mutant, GM71, derived from the doped oligo library contains a transition and a transversion within the same triplet codon. (GTG → CCG in GM71 encodes a Val → Pro substitution, which could not be achieved by mutation of a single base.) The collection as a whole contains more substitutions at AT bases pairs than at GC base pairs. This is due to the fact that the Mutazyme enzyme (which targets GC base pairs) has a higher fidelity and produces fewer mutants than the Taq enzyme.

Overall, $\sim 10^6$ clones were screened. Since the number of possible 42 residue sequences containing one, two or three amino acid substitutions is vastly larger than 10^6, the experimental library could not have included all possible single, double and triple mutants. Nonetheless, since the mutations were produced randomly, the sequences isolated by the fluorescence-based screen represent an unbiased sampling of those amino acid substitutions that reduce the propensity of Aβ42 to form insoluble aggregates.

Characterization of wild type and mutant Aβ peptides

The experiments described above were performed on fusions of Aβ42 to GFP. It seems reasonable to expect that the effects of mutations in the Aβ42 sequence on the solubility of the fusion protein would mirror the effects of such substitutions on the biologically relevant 42-residue peptide. To validate this expectation, we studied the aggregation properties of 42-residue peptides prepared by solid phase synthesis. Specifically, we compared synthetic 42-mers corresponding to the sequences with the lowest (wild-type) and highest (Phe19 → Ser, Leu34 → Pro = GM6) fluorescence *in vivo*, and demonstrated that they have dramatically different propensities for aggregation *in vitro*.

Solubility

Peptide solubility was compared in four different aqueous solutions (Table 2). Lyophilized

Table 1. Frequency of each type of DNA base change in the three individual collection of Aβ42 mutants, and for the entire collection shown in Figure 2

	Taq polymerase	Mutazyme polymerase	Doped oligos	Entire collection
A → G, T → C	32	2	17	51
G → A, C → T	2	2	4	8
Total transitions	34	4	21	59
A → T, T → A	12	5	6	23
A → C, T → G	5	0	12	17
G → C, C → G	1	0	4	5
G → T, C → A	1	2	7	10
Total transversions	19	7	29	55

Table 2. Solubilities of wild-type Aβ42 and the GM6 mutant

	Turbidity (330 nm)		Pellet formation	
	wt Aβ42	GM6	wt Aβ42	GM6
10 mM PBS	0.372	0.021	Yes	Slight
10 mM PB	0.275	0.010	Yes	No
Water	0.318	0.014	Yes	No
1 M Acetic acid	0.002	0.009	No	No

Wild-type Aβ42 is not soluble in aqueous buffer solutions and could only be dissolved in 1 M acetic acid. In contrast, the GM6 mutant was soluble immediately in all solvents (a very small pellet was detectable after centrifugation only in the PBS sample).

peptides were dissolved in water, phosphate buffer (PB), phosphate buffer containing 150 mM NaCl (PBS), or 1 M acetic acid. GM6 was immediately soluble in all four solvents as assessed by turbidity measurements and the presence or absence of a pellet following centrifugation. In contrast, the wild-type peptide was completely soluble only in 1 M acetic acid.

Time-dependent aggregation

Since aggregation phenomena sometimes require periods of incubation, we monitored the turbidity of peptide solutions (0.4 mg/ml, in PBS (pH 7.4)) as a function of time. (We chose PBS rather than PB because in the absence of salt GM6 showed no evidence of aggregation—Table 2.) Lyophilized peptides were dissolved first in 1 M acetic acid (2.5 mg/ml) to disrupt pre-aggregated material. Samples were then centrifuged at 15,000*g* for 10 min, titrated to neutral pH with NaOH, and diluted to 0.4 mg/ml (90 μM) in PBS (pH 7.4). Samples containing the wild-type peptide became turbid immediately after the pH was adjusted to 7.4. In contrast, neutralization of GM6 solution did not cause turbidity (Table 2). Following incubation at room temperature for three hours, GM6 was still mostly soluble. The GM6 sample only became turbid after 24 hours of incubation at 37 °C. Even under these stringent conditions, its turbidity was substantially lower than that of the wild-type peptide (Figure 6(a)).

Turbidity is a convenient measure of aggregation; however, turbidity *per se* does not prove that an aggregated structure is amyloid. To compare the amyloid-forming potential of GM6 with wild-type Aβ42, we monitored binding of Congo red. As shown in Figure 6(b), following dilution into physiological buffer, the wild-type peptide assembled rapidly into Congo red stainable material. In contrast, the mutant peptide does not bind Congo red—even after a three hour incubation at room temperature. (Thus, the slight turbidity of GM6 following three hours (Figure 6(a)), must be caused by an aggregate that is not amyloid.) GM6 binds Congo red only after incubation under relatively stringent conditions—24 hours at 37 °C. Even under these conditions the amount of Congo red bound by the mutant is substantially less than that bound by wild-type Aβ42 in three hours at room temperature (Figure 6(b)).

Secondary structure

We assessed the secondary structure of the GM6 peptide by circular dichroism (CD) spectroscopy. The CD spectrum of GM6 in PB (Figure 7) demonstrates that the mutant peptide does not form a predominantly β-sheet conformation. (The canonical CD spectrum for β-structure has a single minimum at 217 nm[37]) We analyzed the GM6 spectrum using three different secondary structure prediction programs (see Materials and Methods). All three algorithms suggest the secondary structure of GM6 is approximately 18–23% α-helix, 30–32% β-sheet, 20–22% turn, and 28–35% random coil. This contrasts significantly with the predominately β-sheet structure described in the literature for wild-type Aβ42 in amyloid fibrils or as a transient monomer.[26,38,39]

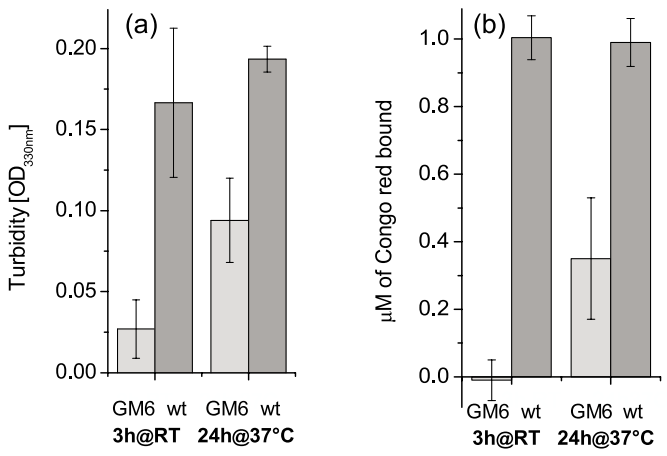

Figure 6. (a) Aggregation of synthetic peptides. Wild-type Aβ42 and GM6 in PBS are compared after three hours at room temperature and an additional 24 hours at 37 °C. Light bars represent GM6 and dark bars represent wild-type Aβ42. (b) Binding of Congo red. The GM6 mutant does not bind Congo red after three hours at room temperature. Thus, the slight turbidity of GM6 following a three hour incubation (Panel A), must be caused by an aggregate that is not amyloid. GM6 binds Congo red only after incubation for 24 hours at 37 °C. Even under these conditions the amount of Congo red bound by GM6 is substantially lower than that bound by wild-type Aβ42 in three hours at room temperature.

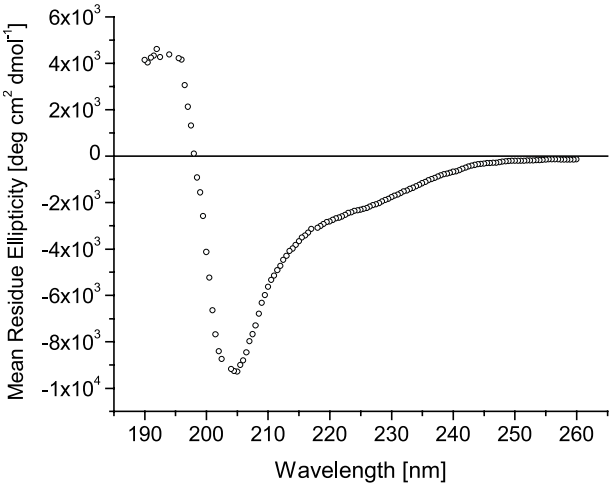

Figure 7. CD spectrum of the synthetic peptide GM6 in 10 mM PB (pH 7.4). Secondary structure analysis programs CONTIN/LL, CDNN and CDSSTR estimate the structure as approximately 18–23% α-helix, 30–32% β-sheet, 20–22% turn and 28–35% "random".

Discussion

Since neither the structure of Aβ amyloid, nor the mechanism of its formation has been elucidated, we devised our screen to enable the isolation of mutants without any preconceived models about which regions of the Aβ sequence might dictate amyloidogenesis. An unbiased and model-independent approach seemed particularly appropriate in light of recent findings by Dobson and co-workers that under appropriate conditions, virtually any polypeptide sequence—including the all α-helical protein myoglobin—can form amyloid-like structures.[40]

Initial application of the screen yielded a collection of 36 variants of Aβ42 (Figure 2). Some of the variants contain single amino acid substitutions, while others contain multiple substitutions. The collection as a whole comprises 94 amino acid substitutions.

Comparison with earlier studies

It is useful to compare the mutations found in our model-independent screen with those designed and constructed in previous studies. The majority (64 out of 94) of the substitutions in our collection occurs in the following short segments: Leu17Val18Phe19, Ile31Ile32, Leu34Met35Val36, and Val39Val40Ile41Ala42. These segments are highly hydrophobic (yellow in Figure 2), and would be expected to facilitate aggregation. The importance of these hydrophobic segments had been suggested by earlier models of Aβ amyloidogenesis.[24–28,41,42]

The central hydrophobic cluster

Several previous studies have implicated the central hydrophobic cluster (Leu17Val18Phe19-Phe20Ala21) as a key determinant of fibrillogenesis.[24,27,28] For example:

(i) A 9-residue peptide comprising these five residues with an additional two residues on either side forms amyloid-like structures.[28] In the context of this 9-mer, replacement of any of these five hydrophobic residues by proline prevents fibril formation and enhances peptide solubility.[28]

(ii) In the context of a synthetic peptide corresponding to Aβ residues 10–43, the substitution of any of the hydrophobic residues at positions 17–20 by more hydrophilic residues reduced aggregation.[27]

(iii) In an *in vivo* system using transgenic *C. elegans*, Fay *et al*.[25] found that the Leu17 → Pro mutation prevents amyloid deposits.

We compare these findings with the current study and note that 18 of the substitutions in our collection occur in residues 17–19. Moreover, three of the singly substituted proteins found in our screen (Leu17 → Glu in GM22, Leu17 → Gln in GM36, and Phe19 → Ser in GM19) owe their green phenotypes to nonpolar → polar substitutions in the central hydrophobic cluster. In particular, position 19 is well-known to affect the folding and assembly of Aβ.[24,26–28] Our collection contains eleven mutations at this position. Mutant GM19 contains a single substitution at this position (Phe19 → Ser); thus, clearly owes its green phenotype to a mutation at position 19.

The hydrophobic clusters in residues 30–36

The hydrophobic regions at 30–32 and 33–36 have also been implicated in earlier studies.[25,29,43] For example:

(i) In the context of a peptide fragment corresponding to residues 25–35 of Aβ, mutation of either Ile31 or Ile32 reduced aggregation.[29] Consistent with these earlier findings, we found that a mutation at either Ile_{31} (to Asn in GM23) or at Ile32 (to Ser in GM1 or to Val in GM21) is sufficient to produce the green phenotype.

(ii) In the context of the full length Aβ42 peptide, Döbeli *et al*.[43] showed that mutation of Gly33Leu34Met35 to Val33Ala34Ala35 decreased aggregation. Consistent with these findings, in our collection of variants, a total of 18 mutations occur at positions 34 and 35. The single mutation Leu34 → Pro (in GM18) is sufficient to yield a green phenotype.

(iii) Position 35 has been implicated as particularly important in studies of several different fragments of Aβ. In the 25–35 fragment, substitution of Met35 by Leu, Lys or Tyr produced peptides unable to form fibrils.[29] Moreover, in the full length Aβ peptide, mutation of Met35 to either Glu, Gln Ser, or Leu reduced aggregation.[43] In the *C. elegans* system, the Met35 → Cys mutation prevented amyloid

deposits.[25] Our screen for green mutants yielded five variants with mutations at Met35.

Overall, 25 of the 36 variants in our collection have at least one substitution in the hydrophobic regions at 30–32, and 34–36.

The C-terminal hydrophobic sequence

Aβ42 is the major component of neuritic plaques.[3,5] Although Aβ40 is produced in greater abundance *in vivo*, the prevalence of the full-length 42-mer in plaques suggests that shorter peptides are less amyloidogenic. Experiments with synthetic peptides have confirmed this expectation: Aβ39 and Aβ40 at 20 μM are kinetically soluble for several days, whereas Aβ42 at the same concentration immediately aggregates into amyloid fibrils.[44,45] These findings suggest that the C-terminal hydrophobic residues of Aβ42 contribute to its amyloidogenicity. Consistent with these earlier results, our screen yielded 11 amino acid substitutions in the C-terminal hydrophobic tetrapeptide. One might question whether fusing GFP to the C terminus of Aβ42 might render it difficult to uncover mutations in the C-terminal residues Ile41 and Ala42. The data in Figure 2 demonstrate this concern is unwarranted: (i) Among the 36 variants, there are seven amino acid substitutions in residues 41 and 42 (as compared to the two mutations found in the N-terminal dipeptide). (ii) The green phenotype is sensitive to mutations in the C-terminal dipeptide: Thus GM33, which contains the two mutations, Leu34 → Pro and Ala42 → Ser, has a higher fluorescence than GM18, which contains only the Leu34 → Pro substitution. This shows that the screen can indeed 'see' effects resulting from mutations in the C-terminal residue (Ala42).

Overall, 54 of the 94 amino acid substitutions in our collection occur in the three hydrophobic stretches implicated in previous studies of Aβ fibrillogenesis.

The full-length Aβ 42-mer is difficult to manipulate (and expensive to synthesize). Consequently, earlier studies of Aβ fibrillogenesis often relied on synthetic peptides containing only part of the Aβ42 sequence.[24,26–29,42] Some of these model peptides comprised as few as nine residues of Aβ.[28] It is reasonable to question whether the sequence determinants implicated by studies of fragments are the same as those responsible for the amyloidogenenic propensity of full-length Aβ42. Our finding that mutations in these three hydrophobic stretches reduce the aggregation of fusions to full length Aβ42 validates these earlier studies.

An unbiased search for the sequence determinants of Aβ amyloidogenesis

Although many of the substitutions shown in Figure 2 are consistent with previous studies, application of the new screen also yielded solubility-enhancing variants that would not have been predicted by previous models of Aβ amyloidogenesis. For example, GM29 (Ala2 → Ser) and GM35 (His6 → Leu, Gly38 → Asp) do not contain any substitutions in the hydrophobic segments mentioned above. Two other variants GM21 (Ile32 → Val) and GM76 (Val18 → Ala, Phe19 → Leu) contain substitutions in these hydrophobic segments, but the substitutions are conservative. Simple models based solely on sequence hydrophobicity would not have predicted that these mutations would enhance solubility. The ability of the screen to uncover novel mutations not predicted by previous models highlights the importance of using an unbiased screen to elucidate the sequence determinants of Aβ amyloidogenicity.

Materials and Methods

Construction of a synthetic gene encoding wild-type Aβ42

The synthetic gene encoding Aβ42 was constructed from two oligonucleotides (Integrated DNA Technologies, Coralville, IA). The sequences of these oligonucleotides were 5′- C TGG GTG ACC CAT ATG GAT GCG GAA TTT CGC CAT GAT TCT GGC TAT GAA GTG CAT CAT CAG AAA CTG *GTG TTT TTT GCG GAA GAT GTG*-3′ and 5′-CT GCA GGA TCC CGC AAT CAC CAC GCC GCC CAC CAT CAG GCC AAT AAT CGC GCC TTT GTT AGA GCC *CAC ATC TTC CGC AAA AAA CAC*-3′.

The two oligonucleotides were annealed together using complementary sequences at their 3′ ends (italics), and second strand synthesis was accomplished using Klenow DNA polymerase (New England Biolabs). Following second strand synthesis, DNA was digested at the *Nde*1 and *Bam* H1 restriction sites (underlined) bracketing the synthetic Aβ sequence. The gene was then inserted into the *Nde*1/*Bam* H1 cloning site of the GFP fusion vector provided by Waldo.[31]

Mutagenesis of Aβ42

Three methods of random mutagenesis were used.

Error prone PCR using Taq polymerase

Error-prone PCR was performed on the Aβ42 gene using the following synthetic oligonucleotide primers: GFP-rev: 5′-AAG TTC TTC TCC TTT GCT GAA-3′ and T7 primer: 5′-TAA TAC GAC TCA CTA TAG GG-3′. Reaction mixtures contained 10 mM Tris–HCl (pH 9.0), 50 mM KCl, 0.1% Triton X-100, 5 mM $MgCl_2$, 0–0.5 mM $MnCl_2$, unbalanced nucleotide concentrations (0.2 mM and 1 mM), various amounts of linearized template plasmid (30–100 ng), 10 pmol primers T7 and GFP-rev, and 2.5 U *Taq* DNA polymerase (Promega) in a total volume of 100 μl. The PCR reaction was performed in an Ericomp Easycycler™ Twinblock™ system with one cycle at 94 °C for one minute; 30 cycles at 94 °C for one minute, 50 °C for one minute, and 72 °C for three minutes; and a final cycle at 72 °C for seven minutes. PCR products were purified using a Qiagen

PCR purification kit, subjected to digestion with the restriction enzymes BamHI and NdeI (New England Biolabs), gel purified, and cloned into the GFP fusion vector.

Error prone PCR using the GeneMorph™ kit

The Mutazyme polymerase used in the GeneMorph™ PCR mutagenesis Kit (Stratagene) has the opposite target bias relative to *Taq* DNA polymerase. Whereas *Taq* is known to target AT base-pairs ~threefold more frequently than GC base-pairs,[34] the Mutazyme polymerase targets GC ~threefold more frequently than AT.[35] Conditions used for the GeneMorph™ PCR mutagenesis were 1× Mutazyme reaction buffer, 200 μM dNTP, various amounts of linearized template plasmid (2–80 ng), 10 pmol primers T7 and GFP-rev, and 2.5 U Mutazyme DNA polymerase in a total volume of 50 μl.

Mutatgenesis using doped oligonucleotides

The third library was constructed from synthetic oligonucleotides in which random mutations were incorporated in the oligonucleotide synthesis. The doped gene was constructed using methods similar to those used to synthesize the wild-type Aβ42 gene, except that bases in the coding region contained 97% of the correct base and 1% of each incorrect base. In the following DNA sequences (Integrated DNA Technologies), doped positions are indicated by small case letters:

5′-C TGG GTG ACC CAT ATG gat gcg gaa ttt cgc cat gat tct ggc tat gaa gtg cat cat cag aaa ctg *gtg ttt ttt gcg gaa gat gtg*-3′ and 5′-CT GCA GGA TCC cgc aat cac cac gcc gcc cac cat cag gcc aat aat cgc gcc ttt gtt aga gcc *cac atc ttc cgc aaa aaa cac*-3′, Second strand synthesis, restriction digestion, and cloning into the GFP fusion vector were performed as described for the wild-type gene (above).

In some cases, second strand synthesis was performed after mixing a doped oligonucleotide encoding one half of the Aβ gene with a wild-type oligonucleotide encoding the other half of the gene. This strategy yielded Aβ variants with mutations in either the first half or the second half of the gene (e.g. GM74, GM76, GM77 and GM79).

Screening for fluorescent colonies

Libraries of mutant plasmids were transformed into XL1-Blue electrocompetent cells (Stratagene) and plated onto LB plates containing 35 μg/ml kanamycin. Colonies were pooled, plasmids were prepared, and then transformed into BL21(DE3) (Stratagene) by electroporation. Cells were plated onto nitrocellulose membranes (Millipore NC-HATF 83 mm) on LB plates containing 35 μg/ml kanamycin. Cells were plated at a density of ~2000 colonies/plate, and grown for 10–12 hours at 37 °C. Membranes where then transferred to LB + kanamycin plates containing 1 mM IPTG and induced for 3 hours at 37 °C. Green fluorescent colonies were picked and plasmid DNA was extracted (Wizard® Plus Miniprep DNA purification system, Promega) and submitted for sequence analysis (Princeton University Syn/Seq facility).

Expression, fluorescence, and solubility of the Aβ42–GFP fusions

Expression

BL21(DE3) cells harboring wild type or mutant Aβ42–GFP fusions were grown at 37 °C in LB medium containing 35 μg/ml kanamycin. When cultures reached an $A_{600\,nm}$ of 0.6, protein expression was induced with 1 mM IPTG. Cultures were grown for an additional three hours and harvested by centrifugation. Expression of Aβ–GFP fusion proteins was monitored by SDS-PAGE: 100 μl of cell culture were pelleted in a 1.5 ml Eppendorf tube, resuspended in 10 μl 10 M urea and 10 μl polyacrylamide gel loading buffer, heated at 100 °C for ten minutes and centrifuged for 15 minutes at 15,000*g*. The supernatant was loaded onto a 8–25% (w/v) acrylamide gel (Amersham Pharmacia Phastsystem) and analyzed by SDS-PAGE.

Fluorescence

Emission spectra of cells expressing wild type and mutant Aβ–GFP were measured on a Perkin–Elmer LS 50 B spectrofluorimeter. Bacterial cultures were grown and induced as above. After three hours of induction, cells were diluted with 10 mM Tris–HCl (pH 7.5) to an $A_{600\text{-}nm} = 0.150$, and the fluorescence emission spectrum of the cell suspension was recorded from 500 to 600 nm, using an excitation wavelength of 490 nm (emission and excitation slits widths 1 mm). Data were corrected for buffer signals and represent unsmoothed scans.

Protein solubility

Cultures were grown and induced as described above. After three hours of induction, 100 μl of cells were harvested by centrifugation. Recombinant proteins were released from the bacterial cytoplasm by resuspending the pellets in 10 μl lysis buffer (50 mM Tris–HCl (pH 7.5), 150 mM NaCl, 10% (v/v) glycerol) containing 1 mg/ml lysozyme, and incubation on ice for 30 minutes followed by four cycles of freeze/thaw. After removal of insoluble proteins and cell debris by centrifugation, supernatant (soluble fraction) and pellet (insoluble fraction) were subjected to SDS-PAGE analysis.

Characterization of synthetic peptides

Synthetic peptides

Wild-type Aβ42 was purchased from Biopeptide Co., San Diego, CA. GM6 ($Phe_{19} \rightarrow Ser$, $Leu_{34} \rightarrow Pro$) was purchased from Sigma Genosys, Woodlands, TX. Purity and identity were verified by mass spectrometry.

Solubility

Mutant or wild-type peptides (of 0.4 mg) were suspended in 1 ml of (a) deionized water, (b) 10 mM PB (pH 7.4), (c) 10 mM PB (pH 7.4) containing 150 mM NaCl (PBS) or (d) 1 M acetic acid. Solubility was assessed by measuring turbidity at 330 nm, and by visually detecting the presence or absence of a pellet after centrifugation at 15,000*g* for ten minutes.

Time course of aggregation

Peptides were solubilized in 1 M acetic acid at concentrations of 2.5 mg/ml and centrifuged at 15,000*g* for ten minutes. These peptide stock solutions were then adjusted to neutral pH with NaOH and diluted to a working concentration of 0.4 mg/ml in 10 mM PB (pH 7.4) containing 150 mM NaCl (PBS). Samples were set up in triplicate (for GM6) and duplicate (for wild-type Aβ42) and incubated for three hours at room temperature and an additional 24 hours at 37 °C.

Congo-red binding

Amyloid formation was monitored by adding 40 μl of a resuspended aggregation sample to 920 μl of a 20 μM Congo-red solution in 10 mM PB (pH 7.4) containing 150 mM NaCl. After 30 minutes incubation at room temperature, the absorbance was measured at 540 and 480 nm, and the concentration of Congo-red bound to fibril was calculated using the equation:

$$C_{\text{bound}}\ (\mu\text{M}) = A_{540}/25,295 - A_{480}/46,306$$

Data were corrected for the signal of 40 μl PBS in 920 μl Congo-red solution (-0.13 ± 0.07 μM). In addition, turbidity of the samples was determined by measuring the absorbance at 330 nm.

CD spectroscopy

GM6 samples were dissolved in 10 mM PB (pH 7.4) to a final concentration of 0.5 mg/ml and incubated overnight at 4 °C. Samples were centrifuged at 15,000*g* for ten minutes prior to CD measurements; however, no aggregated material was detected. Spectra were recorded from 260 to 190 nm on an Aviv 62 DS spectropolarimeter at 25 °C in a 0.1 cm cuvette. Five scans were averaged, smoothed and corrected for buffer signal. Deconvolution of the spectrum was achieved using the program CDNN (version 2.1, 1997).[46] In addition, peptide secondary structure was predicted using the CONTIN/LL program,[47] which is a modified version of the CONTIN algorithm on the basis of the method of Provencher & Glockner,[48] and the CDSSTR program.[47,49]

Acknowledgments

C.W. was supported by a fellowship from the Ministère de la Culture, de L'Enseignement Supérieur et de la Recherche, Grand Duché de Luxembourg. We thank Geoffrey Waldo for the gift of the GFP fusion vector, and Woojin Kim for help with colony screening.

References

1. Koo, E. H., Lansbury, P. T., Jr & Kelly, J. W. (1999). Amyloid diseases: abnormal protein aggregation in neurodegeneration. *Proc. Natl Acad. Sci. USA*, **96**, 9989–9990.
2. Selkoe, D. J. (1991). The molecular pathology of Alzheimer's disease. *Neuron*, **6**, 487–498.
3. Selkoe, D. J. (2001). Alzheimer's disease: genes, proteins, and therapy. *Physiol. Rev.* **81**, 741–766.
4. Wang, R., Sweeney, D., Gandy, S. E. & Sisodia, S. S. (1996). The profile of soluble amyloid β protein in cultured cell media. Detection and quantification of amyloid β protein and variants by immunoprecipitation–mass spectrometry. *J. Biol. Chem.* **271**, 31894–31902.
5. Roher, A. E., Lowenson, J. D., Clarke, S., Woods, A. S., Cotter, R. J., Gowing, E. *et al* (1993). β-Amyloid-(1–42) is a major component of cerebrovascular amyloid deposits: implications for the pathology of Alzheimer disease. *Proc. Natl Acad. Sci. USA*, **90**, 10836–10840.
6. Scheuner, D., Eckman, C., Jensen, M., Song, X., Citron, M., Suzuki, N. *et al* (1996). Secreted amyloid β-protein similar to that in the senile plaques of Alzheimer's disease is increased *in vivo* by the presenilin 1 and 2 and APP mutations linked to familial Alzheimer's disease. *Nature Med.* **2**, 864–870.
7. Weggen, S., Eriksen, J. L., Das, P., Sagi, S. A., Wang, R., Pietrzik, C. U. *et al* (2001). A subset of NSAIDs lower amyloidogenic Aβ42 independently of cyclooxygenase activity. *Nature*, **414**, 212–216.
8. Geula, C., Wu, C. K., Saroff, D., Lorenzo, A., Yuan, M., Yankner, B. A. *et al* (1998). Aging renders the brain vulnerable to amyloid β-protein neurotoxicity. *Nature Med.* **4**, 827–831.
9. Schenk, D., Barbour, R., Dunn, W., Gordon, G., Grajeda, H., Guido, T. *et al* (1999). Immunization with amyloid-β attenuates Alzheimer-disease-like pathology in the PDAPP mouse. *Nature*, **400**, 173–177.
10. Bucciantini, M., Giannoni, E., Chiti, F., Baroni, F., Formigli, L., Zurdo, J. *et al* (2002). Inherent toxicity of aggregates implies a common mechanism for protein misfolding diseases. *Nature*, **416**, 507–511.
11. Walsh, D. M., Klyubin, I., Fadeeva, J. V., Cullen, W. K., Anwyl, R., Wolfe, M. S. *et al* (2002). Naturally secreted oligomers of amyloid β-protein potently inhibit hippocampal long-term potentiation *in vivo*. *Nature*, **416**, 535–539.
12. Glenner, G. G. & Wong, C. W. (1984). Alzheimer's disease: initial report of the purification and characterization of a novel cerebrovascular amyloid protein. *Biochem. Biophys. Res. Commun.* **120**, 885–890.
13. Masters, C. L., Simms, G., Weinman, N. A., Multhaup, G., McDonald, B. L. & Beyreuther, K. (1985). Amyloid plaque core protein in Alzheimer disease and Down syndrome. *Proc. Natl Acad. Sci. USA*, **82**, 4245–4249.
14. Kang, J., Lemaire, H. G., Unterbeck, A., Salbaum, J. M., Masters, C. L., Grzeschik, K. H. *et al* (1987). The precursor of Alzheimer's disease amyloid A4 protein resembles a cell-surface receptor. *Nature*, **325**, 733–736.
15. Zagorski, M. G. & Barrow, C. J. (1992). NMR studies of amyloid β-peptides: proton assignments, secondary structure, and mechanism of an alpha-helix-β-sheet conversion for a homologous, 28-residue, N-terminal fragment. *Biochemistry*, **31**, 5621–5631.
16. Sticht, H., Bayer, P., Willbold, D., Dames, S., Hilbich, C., Beyreuther, K. *et al* (1995). Structure of amyloid A4-(1–40)-peptide of Alzheimer's disease. *Eur. J. Biochem.* **233**, 293–298.
17. Talafous, J., Marcinowski, K. J., Klopman, G. & Zagorski, M. G. (1994). Solution structure of residues 1–28 of the amyloid β-peptide. *Biochemistry*, **33**, 7788–7796.
18. Shao, H., Jao, S., Ma, K. & Zagorski, M. G. (1999). Solution structures of micelle-bound amyloid β-(1–40) and β-(1–42) peptides of Alzheimer's disease. *J. Mol. Biol.* **285**, 755–773.

19. Lee, J. P., Stimson, E. R., Ghilardi, J. R., Mantyh, P. W., Lu, Y. A., Felix, A. M. *et al* (1995). β-Amyloid peptide congeners in water solution. Conformational changes correlate with plaque competence. *Biochemistry*, **34**, 5191–5200.
20. Zhang, S., Iwata, K., Lachenmann, M. J., Peng, J. W., Li, S., Stimson, E. R. *et al* (2000). The Alzheimer's peptide a beta adopts a collapsed coil structure in water. *J. Struct. Biol.* **130**, 130–141.
21. Serpell, L. C. (2000). Alzheimer's amyloid fibrils: structure and assembly. *Biochim. Biophys. Acta*, **1502**, 16–30.
22. Lynn, D. G. & Meredith, S. C. (2000). Review: model peptides and the physicochemical approach to β-amyloids. *J. Struct. Biol.* **130**, 153–173.
23. Chen, S. Y., Harding, J. W. & Barnes, C. D. (1996). Neuropathology of synthetic β-amyloid peptide analogs *in vivo*. *Brain Res.* **715**, 44–50.
24. Esler, W. P., Stimson, E. R., Ghilardi, J. R., Lu, Y., Felix, A. M., Vinters, H. V. *et al* (1996). Point substitutions in the central hydrophobic cluster of a human b-amyloid congener disrupts peptide folding and aolishes plaque competence. *Biochemistry*, **35**, 13914–13921.
25. Fay, D. S., Fluet, A., Johnson, C. J. & Link, C. D. (1998). *In vivo* aggregation of β-amyloid peptide variants. *J. Neurochem.* **71**, 1616–1625.
26. Hilbich, C., Kisters-Woike, B., Reed, J., Masters, C. L. & Beyreuther, K. (1991). Aggregation and secondary structure of synthetic amyloid β A4 peptides of Alzheimer's disease. *J. Mol. Biol.* **218**, 149–163.
27. Hilbich, C., Kisters-Woike, B., Reed, J., Masters, C. L. & Beyreuther, K. (1992). Substitutions of hydrophobic amino acids reduce the amyloidogenicity of Alzheimer's disease β A4 peptide. *J. Mol. Biol.* **228**, 460–473.
28. Wood, S. J., Wetzel, R., Martin, J. D. & Hurle, M. R. (1995). Prolines and amyloidogenicity in fragments of the Alzheimer's peptide β/A4. *Biochemistry*, **34**, 724–730.
29. Pike, C. J., Walencewicz-Wasserman, A. J., Kosmoski, J., Cribbs, D. H., Glabe, C. G. & Cotman, C. W. (1995). Structure-activity analyses of β-amyloid peptides: contributions of the β 25–35 region to aggregation and neurotoxicity. *J. Neurochem.* **64**, 253–265.
30. Fraser, P. E., McLachlan, D. R., Surewicz, W. K., Mizzen, C. A., Snow, A. D., Nguyen, J. T. *et al* (1994). Conformation and fibrillogenesis of Alzheimer A β peptides with selected substitution of charged residues. *J. Mol. Biol.* **244**, 64–73.
31. Waldo, G. S., Standish, B. M., Berendzen, J. & Terwilliger, T. C. (1999). Rapid protein-folding assay using green fluorescent protein. *Nature Biotechnol.* **17**, 691–695.
32. Maxwell, K. L., Mittermaier, A. K., Forman-Kay, J. D. & Davidson, A. R. (1999). A simple *in vivo* assay for increased protein solubility. *Protein Sci.* **8**, 1908–1911.
33. Wigley, W. C., Stidham, R. D., Smith, N. M., Hunt, J. F. & Thomas, P. J. (2001). Protein solubility and folding monitored *in vivo* by structural complementation of a genetic marker protein. *Nature Biotechnol.* **19**, 131–136.
34. Shafikhani, S., Siegel, R. A., Ferrari, E. & Schellenberger, V. (1997). Generation of large libraries of random mutants in Bacillus subtilis by PCR-based plasmid multimerization. *Biotechniques*, **23**, 304–310.
35. Stratagene (2000). *GeneMorph PCR Mutagenesis Kit. Instruction Manual*.
36. Schein, C. H. (1989). Production of soluble recombinant proteins in bacteria. *Bio/Technology*, **7**, 1141–1145.
37. Greenfield, N. & Fasman, G. D. (1969). Computed circular dichroism spectra for the evaluation of protein conformation. *Biochemistry*, **8**, 4108–4116.
38. Barrow, C. J. & Zagorski, M. G. (1991). Solution structures of β peptide and its constituent fragments: relation to amyloid deposition. *Science*, **253**, 179–182.
39. Tomski, S. J. & Murphy, R. M. (1992). Kinetics of aggregation of synthetic β-amyloid peptide. *Arch. Biochem. Biophys.* **294**, 630–638.
40. Fandrich, M., Fletcher, M. A. & Dobson, C. M. (2001). Amyloid fibrils from muscle myoglobin. *Nature*, **410**, 165–166.
41. Soto, C., Castano, E. M., Frangione, B. & Inestrosa, N. C. (1995). The α-helical to β-strand transition in the amino-terminal fragment of the amyloid β-peptide modulates amyloid formation. *J. Biol. Chem.* **270**, 3063–3067.
42. Kirschner, D. A., Inouye, H., Duffy, L. K., Sinclair, A., Lind, M. & Selkoe, D. J. (1987). Synthetic peptide homologous to β protein from Alzheimer disease forms amyloid-like fibrils *in vitro*. *Proc. Natl Acad. Sci. USA*, **84**, 6953–6957.
43. Döbeli, H., Draeger, N., Huber, G., Jakob, P., Schmidt, D., Seilheimer, B. *et al* (1995). A biotechnological method provides access to aggregation competent monomeric alzheimer's 11–42 residue amyloid peptide. *Biotechnology*, **13**, 988–993.
44. Jarrett, J. T., Berger, E. P. & Lansbury, P. T., Jr (1993). The carboxy terminus of the β amyloid protein is critical for the seeding of amyloid formation: implications for the pathogenesis of Alzheimer's disease. *Biochemistry*, **32**, 4693–4697.
45. Jarrett, J. T. & Lansbury, P. T., Jr (1993). Seeding one-dimensional crystallization of amyloid: a pathogenic mechanism in Alzheimer's disease and scrapie? *Cell*, **73**, 1055–1058.
46. Bohm, G., Muhr, R. & Jaenicke, R. (1992). Quantitative analysis of protein far UV circular dichroism spectra by neural networks. *Protein Eng.* **5**, 191–195.
47. Sreerama, N. & Woody, R. W. (2000). Estimation of protein secondary structure from circular dichroism spectra: comparison of CONTIN, SELCON, and CDSSTR methods with an expanded reference set. *Anal. Biochem.* **287**, 252–260.
48. Provencher, S. W. & Glockner, J. (1981). Estimation of globular protein secondary structure from circular dichroism. *Biochemistry*, **20**, 33–37.
49. Johnson, W. C. (1999). Analyzing protein circular dichroism spectra for accurate secondary structures. *Proteins: Struct. Funct. Genet.* **35**, 307–312.

Edited by P. T. Lansbury, Jr

(Received 7 January 2002; received in revised form 3 April 2002; accepted 17 April 2002)